Investigation of the Thermal Properties of $[Cu_{20}Se_{13}(PEt_3)_{12}]$

Andreas Eichhöfer,*[a] Dieter Fenske,[b] and Petra Scheer[a]

Keywords: Cluster compounds / Mixed-valent compounds / Thermogravimetry / Copper / Selenium

The mixed-valence cluster $[Cu_{20}Se_{13}(PEt_3)_{12}]$ has been synthesized by the reaction of CuCl and PEt_3 with $Se(SiMe_3)_2$. A powder-diffraction pattern has revealed its crystalline purity and UV/Vis reflectance spectra display an intervalence band around 1200 nm. The solid-state conversion of the cluster upon heating yields, even at moderate temperatures of around 100 °C, α-Cu_2Se and not a Cu_3Se_2 phase that should be favoured in terms of the Cu/Se ratio of 3.1:2 in the cluster complex. This thermogravimetric analysis, coupled with mass spectrometry, shows that in addition to the labile phosphane ligands selenium atoms are cleaved as $SePEt_3$ during the consolidation process.

Introduction

Cluster molecules of semiconductor materials, composed of tens of atoms with bonding resembling that in the solid state, are interesting molecular models for the bulk.[1] Various cluster molecules of different sizes and structures, composed of elements of either groups 11 and 16 or groups 12 and 16, have been synthesized and characterized by single-crystal XRD.[2−4] Remarkable examples include $[Cd_{32}S_{14}(SPh)_{36}(dmf)_4]$ (dmf = *N*,*N*-dimethylformamide),[5] $[Cu_{146}Se_{73}(PPh_3)_{30}]$,[6] $[Ag_{172}Se_{40}(n\text{BuSe})_{92}(dppp)_4]$ [dppp = bis(diphenylphosphanyl)propane][7] and $[Ag_{188}S_{94}(P\text{n}Pr_3)_{30}]$[8] with cluster core sizes up to 3 nm. Farneth et al. have found that the thermal properties of group 12/16 cluster molecules with the general formula $(R_4N)_4[M_{10}S_4(SPh)_{16}]$ (R = Me, Et; M = Cd, Zn) can give valuable insight into the mechanism of their solid-state conversion upon heating.[9] Investigations on $[Cu_{70}Se_{35}(PEt_2Ph)_{24}]$ reveal that the phosphane ligand shell can be cleaved at moderate temperatures (145 °C) in vacuo in a one-step process that produces nanocrystalline copper selenide.[10] Powder-diffraction measurements show that the cleavage of this ligand molecule is accompanied by an aggregation of the copper selenide cluster cores, in agreement with X-ray photoelectron spectroscopy (XPS) findings on a series of copper selenide clusters.[11] In addition, Corrigan et al. have recently investigated the mechanism of cluster condensation of the copper chalcogenolate $[Cu_6(TePh)_6(PPh_2Et)_5]$ in hexagonally ordered mesoporous MCM-41.[12]

Herein we report the thermal properties of the mixed-valence copper chalcogenide cluster $[Cu_{20}Se_{13}(PEt_3)_{12}]$ and the characterization of its thermolysis products.

Results and Discussion

The reaction of CuCl and PEt_3 with $Se(SiMe_3)_2$ in diethyl ether affords $[Cu_{70}Se_{35}(PEt_3)_{22}]$[13] while only in one experiment a small amount of $[Cu_{20}Se_{13}(PEt_3)_{12}]$ (**1**) crystals were also found. During our investigations it turned out that the use of PTFE gaskets for the stoppers, instead of grease, in combination with evacuation of the flask containing the reaction solution before refrigeration leads to the crystallization of pure **1** (Scheme 1). Obviously, the gaskets were not totally closed, allowing small amounts of oxygen and moisture to enter the flask which could affect an in situ partial oxidation of Se^{2-} to Se^{1-} or Cu^{1+} to Cu^{2+}, respectively. However, attempts to synthesize **1** by the use of an appropriate amount of $CuCl_2$ or $Cu(OOCCH_3)_2$ failed.

$$\begin{array}{l} \text{CuCl + 3 PEt}_3 \\ \text{Et}_2\text{O / −10 °C} \quad \Big| \quad \text{+ 0.5 Se(SiMe}_3)_2 \text{ / } n\text{O}_2 \\ \\ [Cu_{20}Se_{13}(PEt_3)_{12}] \quad \textbf{(1)} \end{array}$$

Scheme 1

The lattice constants of the black octahedral crystals of **1** correspond to those published[13] and the powder-diffraction pattern agrees well with the calculated values, suggesting a high crystalline purity with respect to the formation of other crystalline clusters namely $[Cu_{70}Se_{35}(PEt_3)_{22}]$

[a] Institut für Nanotechnologie, Forschungszentrum Karlsruhe, Postfach 3640, 76021 Karlsruhe, Germany
Fax: (internat.) + 49-7247-82-6368
E-mail: eichhoefer@int.fzk.de
[b] Institut für Anorganische Chemie der Universität Engesserstrasse, Geb. 30.45, 76128 Karlsruhe, Germany

Table 1. Calculated and measured powder-diffraction patterns for $[Cu_{20}Se_{13}(PEt_3)_{12}]$ (**1**) with $I(rel.) > 0.5$

Calculated			Measured		
d [Å]	2Θ [°]	I(rel.)	d [Å]	2Θ [°]	I(rel.)
13.31	6.64	100.00	13.33	6.63	100.00
11.52	7.67	39.73	11.56	7.64	40.84
8.15	10.85	1.05	8.18	10.80	0.89
6.95	12.73	0.60	6.98	12.67	0.97
5.29	16.75	2.63	5.32	16.67	3.00
5.15	17.19	4.84	5.18	17.10	7.28
4.71	18.85	0.53	4.73	18.74	0.90
			4.46	19.88	0.57
4.07	21.80	3.32	4.10	21.67	4.33
3.90	22.81	0.68	3.92	22.68	1.35
3.52	25.32	0.55	3.54	25.17	0.96
3.48	25.62	0.29	3.50	25.46	0.64
3.33	26.78	0.74	3.35	26.61	1.59
3.20	27.89	0.30	3.22	27.72	0.73
3.08	28.97	4.64	3.10	28.79	5.97
3.00	29.75	1.53	3.02	29.56	2.37
2.88	31.02	0.43	2.90	30.82	0.73
2.82	31.75	1.29	2.84	31.56	1.69
2.80	32.00	1.62	2.81	31.79	1.79
2.72	32.95	0.59	2.73	32.74	0.73
2.66	33.65	0.64	2.68	33.43	1.01
2.64	33.88	0.77	2.68	33.44	0.98
			2.66	33.66	0.98
2.58	34.79	0.60	2.59	34.57	0.82
2.53	35.45	2.71	2.55	35.22	2.71
2.42	37.18	2.54	2.43	36.94	2.04
2.32	38.85	0.58	2.33	38.59	0.64
2.26	39.86	2.83	2.28	39.59	2.08
2.23	40.45	0.44	2.23	40.37	1.92
2.22	40.65	2.41			
2.15	42.00	1.59	2.16	41.72	1.37
2.14	42.20	2.28	2.15	41.90	1.86
2.08	43.51	2.47	2.09	43.21	1.89
2.04	44.43	0.88	2.05	44.13	0.93
2.01	44.98	2.61	2.03	44.68	1.93

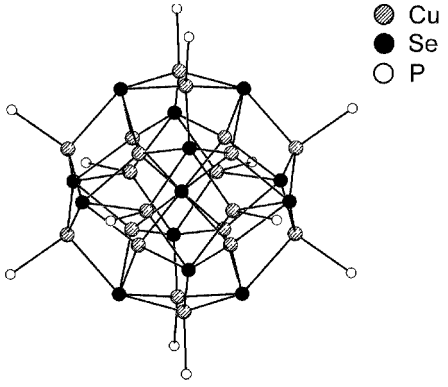

Figure 1. Molecular structure of $[Cu_{20}Se_{13}(PEt_3)_{12}]$ (**1**);[13] copper−copper contacts and carbon and hydrogen atoms omitted for clarity

(Table 1). In the molecular structure of **1** (Figure 1) 13 selenium atoms form a distorted, centered icosahedron (nonbonding Se−Se distances: 4.001−4.143 Å). Twelve of the 20 Se_3 faces are bridged by copper−phosphane units, whereas eight more copper atoms are below the remaining faces, all tetrahedrally surrounded due to an additional Cu−Se bond to the central selenium atom. Assuming a formal charge of 2− for the selenium atoms, one can assign 14 Cu^+ centers and six Cu^{2+} centers. However, the coexistence of Cu^{2+} and Se^{2-} is thermodynamically unlikely because of an electron-transfer process from the reducing Se^{2-} ligand to the oxidizing Cu^{2+} center. Additionally, the electron deficiency has to be assumed to be delocalised as there is no structural reason for it to be localised on either six of the copper atoms or on six of the selenium atoms. The compound should therefore better be described in terms of a "pure" Cu^+ substructure ligated by selenium atoms with an average charge of −1.54.

Compounds containing metal atoms in formally different oxidation states generally exhibit interesting spectroscopic behaviour. Depending on the degree of charge delocalisation in the molecular framework, one may detect additional bands in the near IR. The UV/Vis reflectance spectrum of **1** (Figure 2) shows several bands between 700 and 300 nm. The band with a maximum at 550 nm and a shoulder at 592 nm is responsible for the dark purple colour of the compound while the absorption peak at 262 nm originates most probably from charge-transfer transitions of the PEt_3 ligands. However, the broad, intense peak centered around 1200 nm can be assigned as an intervalence band, in agreement with observations made for similar copper telluride clusters.[14] According to the classification of Robin and Day,[15] which describes the different amounts of electron delocalisation between the metal atoms, **1** belongs to class IIIa (metal clusters). In this class, metal centers with different valencies cannot be distinguished, and total delocalisation of the charge is achieved.

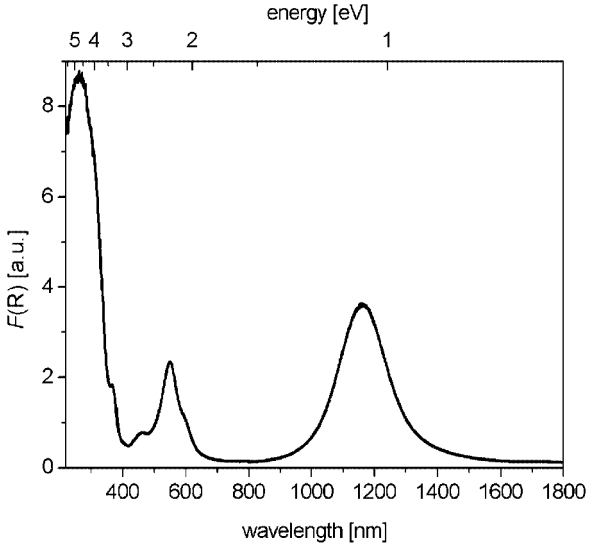

Figure 2. UV/Vis reflectance spectrum of $[Cu_{20}Se_{13}(PEt_3)_{12}]$ (**1**)

Thermogravimetric analysis of **1** in vacuo shows a one-step weight loss of 45.1% centered at 71.5 °C (Figure 3, b). As the cleavage of all the phosphane ligands leads only to

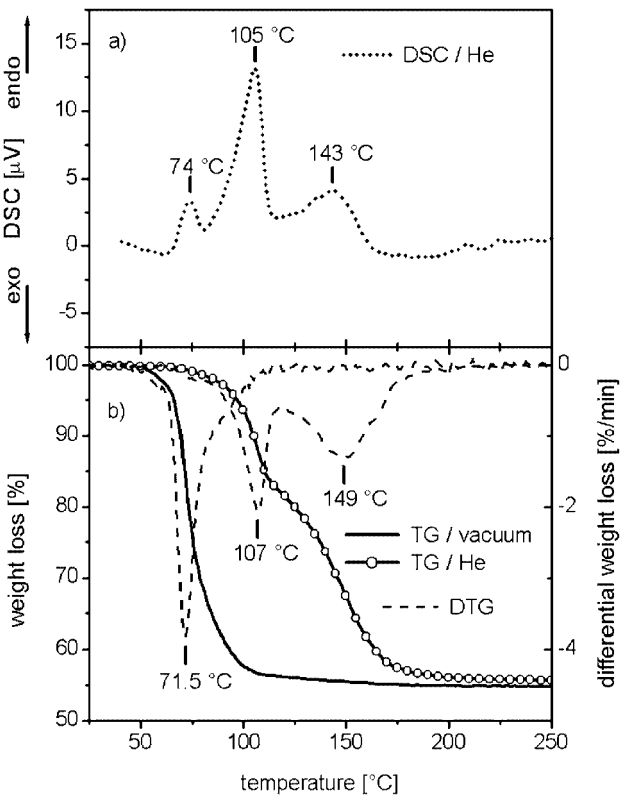

Figure 3. (a) Differential scanning calorimetry of **1**; (b) thermogravimetric analysis of $[Cu_{20}Se_{13}(PEt_3)_{12}]$ (**1**) in vacuo (straight line) and with helium flow (line with circles), the corresponding differential thermogravimetric curves are drawn as dashed lines

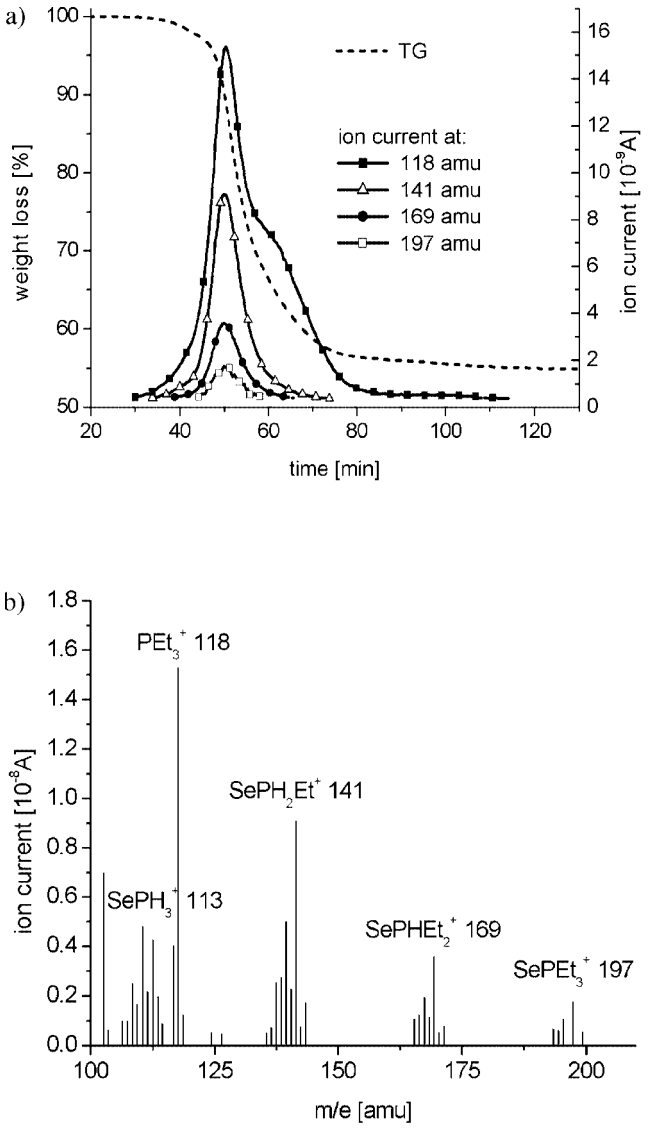

Figure 4. (a) Thermogravimetric analysis of $[Cu_{20}Se_{13}(PEt_3)_{12}]$ (**1**) in vacuo (dashed line) and ion current versus measuring time at 118, 141, 169 and 197 amu; (b) simultaneously recorded mass spectrum of the cleavage products from the thermogravimetry of **1** at cycle 131 (ca. 50 min measuring time)

a theoretical weight loss of 38.2% there appears to be additional elimination of selenium. This was confirmed by simultaneously recorded mass spectra that show peaks attributable to $SePEt_3$ and its fragmentation products (Figure 4, b). The course of the ion current caused by these species (Figure 4, a) indicates that they are formed at an early stage of the cleavage process. In contrast, the ion current for PEt_3 is spread over the whole cleavage process. Theoretical cleavage of three selenium atoms and twelve PEt_3 molecules would lead to a weight loss of 44.5%, which is close to the experimental value. Further evidence for this assumption comes from elemental analysis of the black residue obtained from the TGA, in which the Cu/Se ratio was found to be 1.97:1, in contrast to 3.1:2 in the cluster complex. The analysis further yields C 0.55%, H 0.12%, P $<$ 0.1%.

Thermogravimetric analysis of **1** in a dynamic helium gas flow showed that the thermal decomposition occurs in two successive steps, with maxima in the DTG curve at 107 and 149 °C and weight losses of approximately 17 and 27.4% (Figure 3, b). Here, the change of atmosphere increases the mean cleavage temperature, as has been observed previously for $[Cu_{70}Se_{35}(PEt_2Ph)_{24}]$.[10] The simultaneously recorded mass spectra of the volatile products show only the appropriate peaks for PEt_3 from the beginning of the first step but not for $SePEt_3$ at any stage of the cleavage process. This originates from the use of a TG-MS skimmer coupling system under normal pressure, which reduces the amount of substances reaching the detector and thus the intensity of the signal in comparison with measurements in vacuo. However, the formation of $SePEt_3$ in this case was proven by ^{31}P NMR in C_6D_6 [δ = 44.55 (m) ppm][16] and GC-MS of the collected cleavage products from a cold trap.

A more detailed investigation of the two cleavage steps suggests that in the first step only PEt_3 is cleaved and no $SePEt_3$, due to the different boiling points of the two compounds. In agreement, elemental analysis of the product at approximately 17% mass loss shows C 14.7% and H 3.1%, corresponding to the theoretical cleavage of five PEt_3 molecules (16% weight loss) which would lead to $Cu_{20}Se_{13}(PEt_3)_7$ (C 16.14%, H 3.4%) while the cleavage of three $SePEt_3$ molecules (15.6% weight loss) would give $Cu_{20}Se_{10}(PEt_3)_9$ (C 20.8%, H 4.4%). Furthermore, the cleavage of

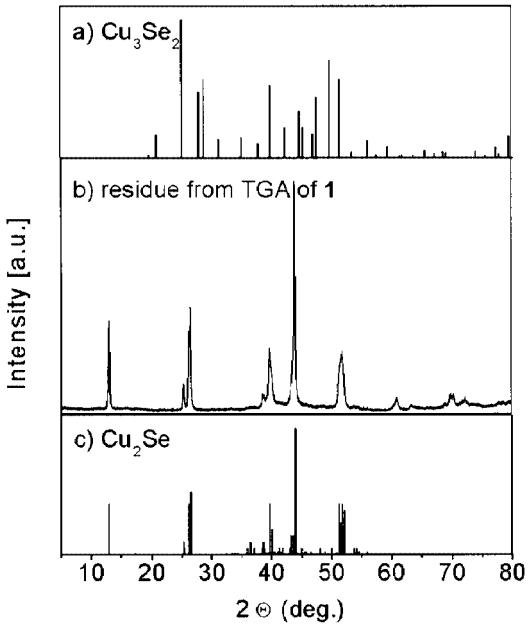

Figure 5. Room-temperature powder-diffraction patterns of (a) Cu_3Se_2;[19] (b) residue of the thermogravimetric analysis of $[Cu_{20}Se_{13}(PEt_3)_{12}]$ (**1**) in vacuo and (c) monoclinic α-Cu_2Se from ref.[18]

$SePEt_3$ in the second step can just be observed by eye upon careful stepwise heating of **1** in a glass flask and is indicated by the sudden formation of white needles on the flask walls above 100 °C. In the powder-diffraction pattern of the intermediate product (heated to 120 °C, 17% mass loss) we found no reflections due to the reported structure of Cu_3Se_2[17] but rather broad reflections pointing to the formation of Cu_2Se[18] (see discussion of powder-diffraction patterns below). Additionally, we found sharp peaks that agree with the calculated pattern of $SePEt_3$.[19] Thus, at almost below 100 °C, phosphane selenide is formed, in agreement with the vacuum TGA, but due to its higher boiling point under normal pressure it escapes from the crucible in the second step.

The differential scanning calorimetry (DSC) curve displays three separated peaks that correspond to three endothermal events in the sample under normal pressure in a dynamic helium gas flow. While the peaks at 105 and 143 °C agree with the two weight-loss steps in thermogravimetry the first endothermal reaction, centered around 74 °C, is more complicated. As the determination of the melting point of the sample gives no evidence for a related process of **1** at this temperature we suggest that the onset of the DSC signal (64 °C) depicts the limit of the thermal stability of **1**. Further heating leads to a decomposition of **1** induced by the formation of $SePEt_3$, a process that is thus clearly separated from the mass loss generated by the escape of PEt_3 and $SePEt_3$ from the crucible.

The powder-diffraction pattern of the thermogravimetric residues of **1** after heating to 250 °C are similar for measurements both in vacuo and in a helium gas flow. The peak positions (Figure 5) agree well with those reported for monoclinic α-Cu_2Se.[18] Furthermore no formation of a Cu_3Se_2 phase[19] was observed although it should be more favoured according to the Cu/Se ratio of 3.1:2 in the cluster complex. This corresponds, on the one hand, to the composition $Cu_{1.97}Se$ determined by elemental analysis and, on the other hand, to the observed mass reduction in thermogravimetry, which strongly suggests the cleavage of three selenium atoms in addition to the triethylphosphane ligands. Stevels has reported that Cu_3Se_2 disproportionates between 120 and 135 °C to form $Cu_{1.8}Se$ and CuSe.[20] In our case, vacuum conditions and the phosphanes, which allows the formation of volatile $SePEt_3$, obviously further reduces the stability of the Cu_3Se_2 phase, leading to the formation of α-Cu_2Se.

Experimental Section

General: Standard Schlenk techniques were employed throughout the syntheses using a double manifold vacuum line with high-purity dry nitrogen. Diethyl ether was dried with sodium/benzophenone and distilled under nitrogen. Anhydrous CuCl (Fluka) was purified from traces of $CuCl_2$ by subsequent washing with dilute HCl, methanol and diethyl ether followed by drying in vacuo. $Se(SiMe_3)_2$ [21] and PEt_3 [22] were prepared according to standard literature procedures. ^{31}P NMR spectra were recorded with a Bruker DPX Avance 300 with 85% H_3PO_4 as an external standard. The solid-state reflectance spectra were measured with a Varian Cary 500 spectrophotometer as micron-sized crystalline powders between quartz plates with a Labsphere integrating sphere.

$[Cu_{20}Se_{13}(PEt_3)_{12}]$ (1): PEt_3 (1.43 mL, 9.7 mmol) was added to a suspension of CuCl (0.32 g, 3.23 mmol) in diethyl ether (40 mL) and stirred for 1 h to give a clear solution. $Se(SiMe_3)_2$ (0.36 mL, 1.62 mmol) was then added at −40 °C and the flask with the PTFE gaskets as stoppers was evacuated before storage at −20 °C. A successful reaction is indicated by the formation of a violet solution. Then, after warming up to −10 °C, black octahedral crystals of **1** appeared within a few days with a final total yield of 20%. $C_{72}H_{180}Cu_{20}P_{12}Se_{13}$ (3715.3): calcd. C 23.28, H 4.88; found C 23.03, H 4.72.

X-ray Crystallography: Crystals suitable for single-crystal X-ray diffraction were obtained directly from the reaction solutions of the compound and then selected in perfluoroalkyl ether oil. Single-crystal X-ray diffraction data for determination of the cell constants of **1** were collected using graphite-monochromatized Mo-K_α radiation (λ = 0.71073 Å) with a STOE IPDS II (Imaging Plate Diffraction System). For more details concerning the crystallographic data of **1**, see ref.[13] The molecular diagram was prepared using the program SCHAKAL 97.[23] X-ray powder-diffraction (XRD) patterns were measured with a STOE STADI P diffractometer (Cu-K_α radiation, germanium monochromator, Debye−Scherrer geometry) in sealed glass capillaries. Theoretical powder-diffraction patterns for **1** were calculated on the basis of the atom coordinates obtained from single-crystal X-ray analysis by using the program package STOE WinXPOW.[24]

Thermogravimetric Analysis: Thermogravimetric analyses were run with a thermobalance STA 409 from Netzsch either in vacuo or with a dynamic helium gas flow (70 mL/min) (heating rate 2 K/min). The balance is coupled with a quadrupole mass spectrometer QMG 422 (Balzers) that includes a skimmer system for measurements under normal pressure.

Acknowledgments

This work was supported by the Deutsche Forschungsgemeinschaft (Center of Functional Nanostructures). We thank Frau Tröster for her valuable assistance in the laboratory.

[1] *Clusters and Colloids* (Ed.: G. Schmid), VCH, Weinheim **1995**.
[2] S. Dehnen, A. Eichhöfer, D. Fenske, *Eur. J. Inorg. Chem.* **2002**, 279−317.
[3] I. Dance, K. Fisher, *Progress in Inorganic Chemistry*, vol. 41 (Ed.: Kenneth D. Karlin), John Wiley & Sons, Inc., New York, Weinheim, **1994**, p. 637−802.
[4] T. Vossmeyer, G. Reck, L. Katsikas, E. T. K. Haupt, B. Schulz, H. Weller, *Science* **1995**, *267*, 1476−1479; T. Vossmeyer, G. Reck, B. Schulz, L. Katsikas, H. Weller, *J. Am. Chem. Soc.* **1995**, *117*, 12881−12882.
[5] N. Herron, J. C. Calabrese, W. E. Farneth, Y. Wang, *Science* **1993**, *259*, 1426−1428.
[6] D. Fenske, H. Krautscheid, G. Baum, M. Semmelmann, *Angew. Chem.* **1993**, *105*, 1364−1367; *Angew. Chem. Int. Ed. Engl.* **1993**, *33*, 1303−1305.
[7] D. Fenske, T. Langetepe, N. Zhu, *Angew. Chem.* **1998**, *110*, 2783−2788; *Angew. Chem. Int. Ed.* **1998**, *37*, 2640.
[8] X.-J. Wang, T. Langetepe, C. Persau, B.-S. Kang, G. M. Sheldrick, D. Fenske, *Angew. Chem.* **2002**, *114*, 3972−3977; *Angew. Chem. Int. Ed.* **2002**, *41*, 3818−3822.
[9] W. E. Farneth, N. Herron, Y. Wang, *Chem. Mater.* **1992**, *4*, 916−922.
[10] A. Eichhöfer, E. Beckmann, D. Fenske, D. Herein, H. Krautscheid, R. Schlögl, *Isr. J. Chem.* **2001**, *41*, 31−37.
[11] D. van der Putten, D. Olevano, R. Zanoni, H. Krautscheid, D. Fenske, *J. Electron. Spectrosc. Relat. Phenom.* **1995**, *76*, 207−211.
[12] C. Kowalchuk, J. F. Corrigan, Y. Huang, *Chem. Commun.* **2000**, 1811−1812.
[13] D. Fenske, H. Krautscheid, *Angew. Chem.* **1990**, *102*, 1513−151; *Angew. Chem. Int. Ed. Engl.* **1990**, *29*, 1452−1454.
[14] A. Eichhöfer, J. F. Corrigan, D. Fenske, E. Tröster, *Z. Anorg. Allg. Chem.* **2000**, *626*, 338−348.
[15] M. B. Robin, P. Day, *Adv. Inorg. Radiochem.* **1967**, *10*, 248−422.
[16] N. Muller, P. C. Lauterbur, J. Goldenson, *J. Am. Chem. Soc.* **1956**, *78*, 3557−3561.
[17] In Powder-diffraction file PDF-2 Database Sets 1−85, **1993**, International Center for Diffraction Data, Newtown Square USA, File number 72−1421; N. Morimoto, K. Koto, *Science* **1966**, *152*, 345; R. MacLaren Murray, R. D. Heyding, *Can. J. Chem.* **1976**, *54*, 841.
[18] In Powder-diffraction file PDF-2 Database Sets 1−85, **1993**, International Center for Diffraction Data, Newtown Square USA, File number 27−1131; A. L. N. Stevels, *Philips Res. Rep. Suppl.* **1969**, *9*, 39−44.
[19] M. van Meerssche, A. Leonard, *Acta Crystallogr.* **1959**, *12*, 1053−1054.
[20] A. L. N. Stevels, *Philips Res. Rep. Suppl.* **1969**, *9*, 44−46.
[21] H. Schmidt, H. Ruf, *Z. Anorg. Allg. Chem.* **1963**, *321*, 270−273.
[22] K. Sasse in *Methoden der Organischen Chemie, Houben-Weyl*, Thieme Verlag, Stuttgart, **1963**, vol. 1, p. 32; H. D. Kaesz, F. G. Stone, *J. Org. Chem.* **1959**, *24*, 635−637.
[23] E. Keller, *SCHAKAL 97, A Computer Program for the Graphic Representation of Molecular and Crystallographic Models*, Universität Freiburg, **1997**.
[24] STOE, *WinXPOW*, STOE & Cie GmbH, Darmstadt, **2000**.

Received May 6, 2003
Early View Article
Published Online October 31, 2003

